

Article

MoO₃ Solubility and Chemical Durability of V₂O₅-Bearing Borosilicate Glass

Minako Nagata and Toru Sugawara *

Graduate School of Engineering Science, Cooperative Major in Sustainable Engineering, Akita University, Akita 010-0852, Japan; m8022936@s.akita-u.ac.jp

* Correspondence: toru@gipc.akita-u.ac.jp

Abstract: In the vitrification of high-level radioactive liquid waste (HLW), the separation of sodium-molybdate melts is a problem because it reduces the chemical durability of the vitrified waste. A glass with both high MoO₃ solubility and chemical durability is required for the safe disposal of radioactive waste. In this study, we investigate the effects of vanadium oxide on the phase separation of the molybdenum-rich phase and the water resistance of the resulting glass by phase equilibrium experiments and chemical durability test. Phase equilibrium experiments were performed on SiO₂-B₂O₃-Al₂O₃-ZnO-CaO-Na₂O-LiO₂-MoO₃ system glasses and on glasses with V₂O₅ added. The results showed that MoO₃ solubility increased when V₂O₅ was added. The increase in MoO₃ solubility in borosilicate melts may be associated with the viscosity-lowering effect of V₂O₅. Chemical durability tests were performed on borosilicate glass compositions obtained from phase equilibrium experiments. The normalized leaching rates of V₂O₅-bearing glasses were higher than those of other glasses. This is due to the higher network modifier/network former ratio of the glass tested. The normalized elemental mass loss of glass containing waste components increases with increasing leaching duration. This suggests that the waste component prevents the formation of a gel layer at the reaction front.

Keywords: glass; high-level radioactive waste; phase separation



Citation: Nagata, M.; Sugawara, T. MoO₃ Solubility and Chemical Durability of V₂O₅-Bearing Borosilicate Glass. *Inorganics* **2023**, *11*, 311. <https://doi.org/10.3390/inorganics11070311>

Academic Editor: Lukáš Krivosudský

Received: 13 June 2023

Revised: 21 July 2023

Accepted: 22 July 2023

Published: 24 July 2023



Copyright: © 2023 by the authors. Licensee MDPI, Basel, Switzerland. This article is an open access article distributed under the terms and conditions of the Creative Commons Attribution (CC BY) license (<https://creativecommons.org/licenses/by/4.0/>).

1. Introduction

High-level radioactive liquid waste (HLW) generated in the spent fuel reprocessing process melts with glass and is geologically disposed of as vitrified waste [1–8]. Glass used for vitrification requires high chemical durability. Many countries, including Japan, plan to use borosilicate glass for HLW vitrification [9–13]. Borosilicate glass is considered durable, easy to manufacture, and capable of homogeneously dissolving various elements.

In the vitrification process of HLW, it is necessary to pay attention to the behavior of molybdenum, which is one of the fission products. Molybdenum has low solubility in silicate melts and separates into borosilicate melts and sodium-molybdate melts by liquid-liquid immiscibility [14] during the melting stage. The molybdenum-rich separated phase, called as the yellow phase (YP), is highly soluble in water and can dissolve various fission products [15]. Therefore, the separation of YP significantly reduces the chemical durability of the vitrified waste [16,17]. The crystallization of the molybdenum phase has been investigated for glasses with various compositions [18–29]. It has been indicated that the solubility of MoO₃ in borosilicate glasses increased with increasing B₂O₃/SiO₂ ratio [19,25,28,29] and decreasing Al₂O₃ content [25,28,29].

In order to improve the solubility of molybdenum in waste glass, the effect of an additive component has also been examined. One of the candidates is vanadium-bearing glass. Manara et al. [30] reported that V₂O₅ added borosilicate glass exhibits a high immobilizing capacity for sulfur containing HLW. Lian et al. [26] indicated that the crystallization tendency of powellite (CaMoO₄) was suppressed in V₂O₅ added borosilicate glasses, and

the molybdenum solubility was improved. Moreover, chemical durability test (PCT) results showed that the normalized leaching rate of V_2O_5 -bearing glass remained at a much lower level than that of standard borosilicate glass. Sugawara et al. [29] indicated that the addition of V_2O_5 accelerates the crystallization of powellite when the glass is slowly cooled ($1\text{ }^\circ\text{C}/\text{min}$). This is the opposite result mentioned by Lian et al. [26], suggesting that cooling rate affects the crystallization tendency of powellite.

Although the crystallization of powellite has been investigated in detail, the effect of vanadium on the phase separation of sodium-molybdate, the main component of YP, has not yet been reported. In this study, we investigated the liquid-liquid immiscibility of V_2O_5 -bearing MoO_3 -rich borosilicate melt by phase equilibrium experiments. We also report the water resistance of the resulting glass through a chemical durability test.

2. Experimental

2.1. Strategy

First, we describe the flow of our experiments using the schematic phase diagram shown in Figure 1. The initial composition of experimental material is C in Figure 1, which is a composition with X mol% MoO_3 added to composition A. When the C is kept at temperature T_1 and equilibrated, it separates into a silicate melt (D) and a molybdate melt (E). The composition F is the normalized composition of D without MoO_3 . Then, the MoO_3 content of D is equal to the MoO_3 solubility of F (Y mol%) under equilibrium conditions.

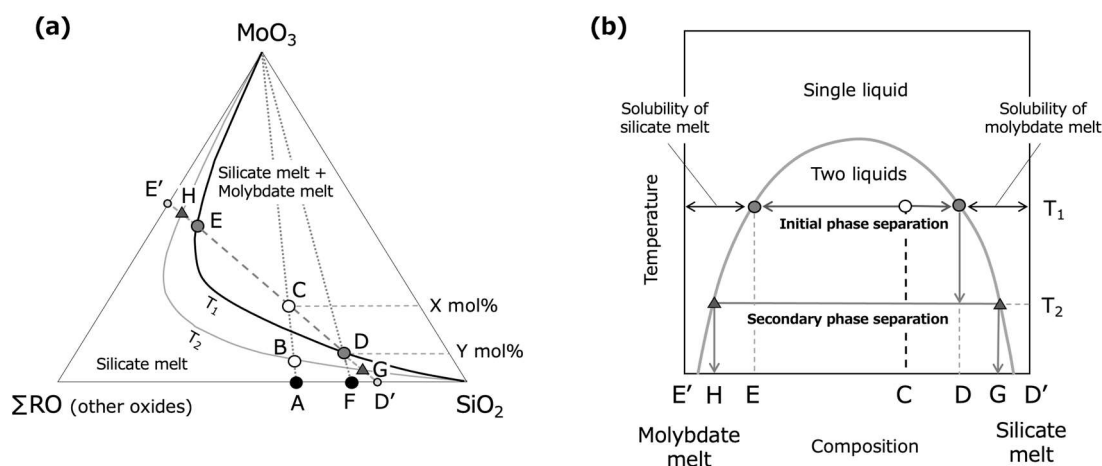


Figure 1. Schematic phase diagram showing immiscibility between silicate liquid and molybdate liquid in (a) the pseudo-ternary system of SiO_2 - MoO_3 - ΣRO (other oxides) estimated from the phase relationship of the SiO_2 - MoO_3 - Na_2O system [31] and (b) the pseudo-binary system between D' and E' in (a). The black solid curve represents the phase boundary between a single liquid and two liquids at temperature T_1 , and the gray curve is at temperature T_2 ($T_1 > T_2$). The initial composition of the phase equilibrium experiments in this study is composition C, which is composition A with X mol% MoO_3 added. Since the C is in the two-phase region, it separates into a silicate melt of composition D and a molybdate melt of composition E when kept at T_1 . The MoO_3 content in composition D (Y mol%) is equal to the saturation solubility of MoO_3 for composition F.

In previous studies [19–24,26,27,29], solubility and crystallization of molybdenum phases have been examined by using glasses with a relatively smaller amount of MoO_3 (<10 wt% or 5 mol%, for example, composition B in Figure 1). In this case, because MoO_3 content is less than equilibrium solubility at temperature (T_1), phase separation and/or crystallization may occur during cooling, even if it is a single liquid at T_1 . The opposite effect of vanadium oxide on the powellite crystallization described above may have been caused by the different cooling rate, quench in [26] and slow cooling in [29].

In contrast, phase equilibrium experiments for the samples with an excess amount of MoO₃ provide equilibrium solubility. Based on those experiments, we have determined the phase separated compositions D and E in the borosilicate systems and used them for the thermodynamic analysis of liquid-liquid immiscibility [25,28]. In this study, we determined equilibrium MoO₃ solubility by phase equilibrium experiments at 1200 °C or 1000 °C for a V₂O₅-bearing borosilicate system.

2.2. Phase Equilibrium Experiments

Chemical composition of starting materials is shown in Table 1.

Table 1. Chemical composition of samples for phase equilibrium experiments (mol%).

Sample	SiO ₂	B ₂ O ₃	Al ₂ O ₃	ZnO	CaO	Na ₂ O	Li ₂ O	V ₂ O ₅	MoO ₃
19A2	39.8	15.4	2.4	1.8	5.3	16.0	6.2	0.0	13.0
21E	38.2	14.8	2.3	1.7	5.3	16.0	6.2	2.4	13.0
21E2	34.6	18.4	2.3	1.7	5.3	16.0	6.2	2.4	13.0

The 19A2 composition is borosilicate glass, which is expected to be used in Japan for HLW vitrification [29,32]. The difference between the 19A2 and glass compositions of Lian et al. [26], who investigated the effect of vanadium, is that our glass has a higher Na₂O/CaO ratio and contains ZnO and Li₂O. The 21E has a composition of 19A2 with V₂O₅ added. The 21E2 has a composition with an increased B₂O₃/SiO₂ ratio compared to the 21E in order to improve the MoO₃ solubility.

Reagent grades SiO₂, B₂O₃, Al₂O₃, ZnO, CaCO₃, Na₂CO₃, Li₂CO₃, V₂O₅, and MoO₃ were weighed and mixed in an agate mortar. The mixed sample was placed in a platinum crucible, covered with an alumina lid, and held in a heating furnace at 1200 °C or 1000 °C for 24 h. Then it was quenched by cooling the bottom of the crucible with water.

After the experiment, the sample separated into upper glass and lower precipitate. A few pieces of glass and precipitate were randomly selected, mounted in epoxy, and polished under oil. Backscattered electron images (BEI) of glass were observed using electro-probe microanalysis (EPMA).

The Li₂O content of experimental samples was analyzed by Inductively Coupled Plasma Atomic Emission Spectroscopy (ICP-AES), B₂O₃ by EPMA, and other elements by X-ray Fluorescence analysis (XRF). For ICP-AES analysis, the sample was crushed, and acid decomposition was performed. The XRF analysis was carried out by the glass bead method.

The amounts (mass %) of phase separated glass, p and precipitate, q were determined by mass-balance calculation. Let x and y be the analytical values of oxide components (mass %) for glass and precipitate, respectively, and X be the initial composition. Then, the p , q and the amount of B₂O₃-loss by volatilization during the experiment, r were obtained by minimizing the residual, σ expressed by the following equation:

$$\sigma = \sqrt{\left(\sum_i \left(\frac{p}{100}x_i + \frac{q}{100}y_i\right) - X_i\right)^2 + \left(\frac{p}{100}x_{B_2O_3} + \frac{q}{100}y_{B_2O_3} + r - X_{B_2O_3}\right)^2}$$

where i represents oxides other than B₂O₃.

Our preliminary experiments confirm that most of the B₂O₃ loss occurs within 6 h, after which the composition of the sample remains constant.

2.3. Chemical Durability Test

A chemical durability test was conducted to investigate the water resistance of the borosilicate glass after phase separation (D in Figure 1). In order to prevent the difference in leaching rate due to the difference in MoO₃ content, Glass compositions were normalized to 100% without MoO₃ (F in Figure 1), and then 2mol% MoO₃, which is lower than the

solubility limit, was added for all glasses. The glass composition is shown in Table 2. For comparison, we also tested simulated HLW glass containing waste components (Bead composition).

Table 2. Chemical composition (mol%) of glasses for the chemical durability test. NF, Sum of network-forming or intermediate oxides ($\text{SiO}_2 + \text{B}_2\text{O}_3 + \text{Al}_2\text{O}_3 + \text{ZnO} + \text{V}_2\text{O}_5$); NM, Sum of network-modifier oxides ($\text{CaO} + \text{Na}_2\text{O} + \text{Li}_2\text{O}$). The glass composition by Lian et al. [26] is also indicated for comparison.

	Sample	SiO ₂	B ₂ O ₃	Al ₂ O ₃	ZnO	CaO	Na ₂ O	Li ₂ O	V ₂ O ₅	MoO ₃	NF	NM
Lian et al. [26]	Vx-M2	58.8	13.9	2.9	0.0	11.2	11.3	0.0	0.0–3.0	2.0	75.5	24.5
This study	19A2	54.7	12.1	3.3	2.4	5.4	14.0	6.1	0.0	2.0	72.5	27.5
	21E	52.2	10.2	3.2	2.3	5.1	13.9	9.0	2.1	2.0	70.0	30.0
	21E2	49.0	13.2	3.3	2.3	5.7	15.5	6.5	2.5	2.0	70.3	29.7
	Bead	51.3	14.4	3.2	2.3	3.8	10.6	8.2	0.0	2.0	71.2	24.5
Waste components in Bead		K ₂ O	MnO ₂	Fe ₂ O ₃	CoO	NiO	ZrO ₂	BaO	La ₂ O ₃	Ce ₂ O ₃	Pr ₂ O ₃	Gd ₂ O ₃
		0.13	0.29	0.37	0.16	0.52	1.20	0.25	0.62	0.35	0.08	0.30

The chemical durability test was conducted in accordance with MCC-3. The glass samples were crushed and sieved to adjust the particle size to 40–75 μm , ultrasonically cleaned in acetone, and dried. For the leaching solution, 1 L of ultrapure water was adjusted to pH 9 (room temperature) using KOH aqueous solution. A Teflon container was placed on a magnetic stirrer with a hot plate, and a thermocouple was attached to the container to measure the experimental temperature. The experiment was conducted at 90 °C. Once the temperature of the leaching solution in the Teflon container stabilized at 90 °C, 0.235 g of glass powder was added to the leaching solution. The solution was stirred during the test, but the water was not replaced. The leachates were collected after 2, 4, 6, 8, 24, 30, and 48 h, and the concentrations of Si and B were investigated using ICP-AES. The normalized leaching rate was obtained from the concentration of the leachate using the following formula,

$$LR_i = \frac{C_i}{f_i \cdot (SA/V) \cdot \Delta t}$$

where LR_i is the normalized leaching rate ($\text{g}/\text{m}^2\text{d}$), C_i is the concentration of element i in the leachate (g/L), f_i is the weight fraction of element i in glass, V is the leachate volume (L), SA is the surface area of the powder sample (m^2), and Δt is the experiment time (days). The SA was determined using a surface area analyzer in BET nitrogen adsorption. The SA was approximately $0.5 \text{ m}^2/\text{g}$ and the SA/V ratio was approximately 118 m^{-1} .

3. Results and Discussion

3.1. Phase Separation of Borosilicate Melt and Molybdate Melt

After the experiment, the sample separated into silicate glass in the upper part and a molybdenum-rich precipitate in the lower part (Figure 2). It is considered that the glass in the upper part corresponds to the HLW glass, and the precipitates can be regarded as simulated YP. As for the appearance of the glass, 19A2 was white, and 21E and 21E2 were slightly yellowish. The precipitate of 19A2 was ivory and more brittle than glass, and those of 21E and 21E2 were ochre and slightly harder than that of 19A2.

Figure 3 shows backscattered electron images of the glass and precipitate. Spherical particles and holes with a diameter of about 1–3 μm were observed in the glass. They were higher at 1200 °C than at 1000 °C and more pronounced at 21E and 21E2 than at 19A2. Similar textures has been previously reported in MoO_3 -bearing sodium-rich silicate glasses [29,33].



Figure 2. Appearance of glass and precipitate was observed for 19A2 and 21E compositions after phase equilibrium experiments at 1200 °C.

EPMA analysis indicated the spherical particles were Powellite (CaMoO_4). The white color of the glass (Figure 2) is derived from those powellite particles. These powellites were not originally precipitated at experimental temperatures and are considered to have been formed by nucleation and crystal growth during cooling.

It is likely that the sodium-molybdate phase (Na_2MoO_4 , $\text{Na}_2\text{Mo}_2\text{O}_7$) was also crystallized from molybdate melt formed by secondary phase separation during cooling (H in Figure 1). However, it is speculated that it was lost by polishing and holes were left since Na_2MoO_4 is water soluble (solubility of 653 g/L) [34]. Sugawara et al. [29] reported that the frequency and size of holes on the sample surface are related to the intensity of $\text{Na}_2\text{MoO}_4 \cdot 2\text{H}_2\text{O}$ in bulk glasses measured by XRD.

The fact that there were fewer powellites at 1000 °C than at 1200 °C was due to a decrease in MoO_3 solubility at lower temperatures. Similarly, powellite was more pronounced in 21E2 than in 19A2 at constant temperature (Figure 3), indicating that the addition of V_2O_5 increased MoO_3 solubility.

The precipitates consisted of spherical silicate glass with a diameter of 5–15 μm (black spherical phase in Figure 3) and a molybdate matrix. It is considered that they were molybdate melts at experimental temperatures. The proportion of spherical silicate phase was greater at 1200 °C than at 1000 °C.

3.2. Effect of V_2O_5 on MoO_3 Solubility in Glass

Table 3 summarizes the chemical composition of silicate glass and molybdenum-rich precipitates. B_2O_3 and Al_2O_3 were partitioned into silicate phases, while Na_2O , Li_2O , and V_2O_5 were enriched in molybdate phases. The MoO_3 solubility was 4.3mol% for 19A2 at 1200 °C, increased to 5.6 mol% for 21E and 8.6mol% for 21E2, and decreased with decreasing temperature. The fact that there were fewer powellite crystals at 1000 °C than at 1200 °C was consistent with a decrease in MoO_3 solubility at lower temperatures. Similarly, powellite and spherical holes were more pronounced in 21E2 than in 19A2 at the same temperature (Figure 3). This is also in agreement with the increase in MoO_3 solubility.

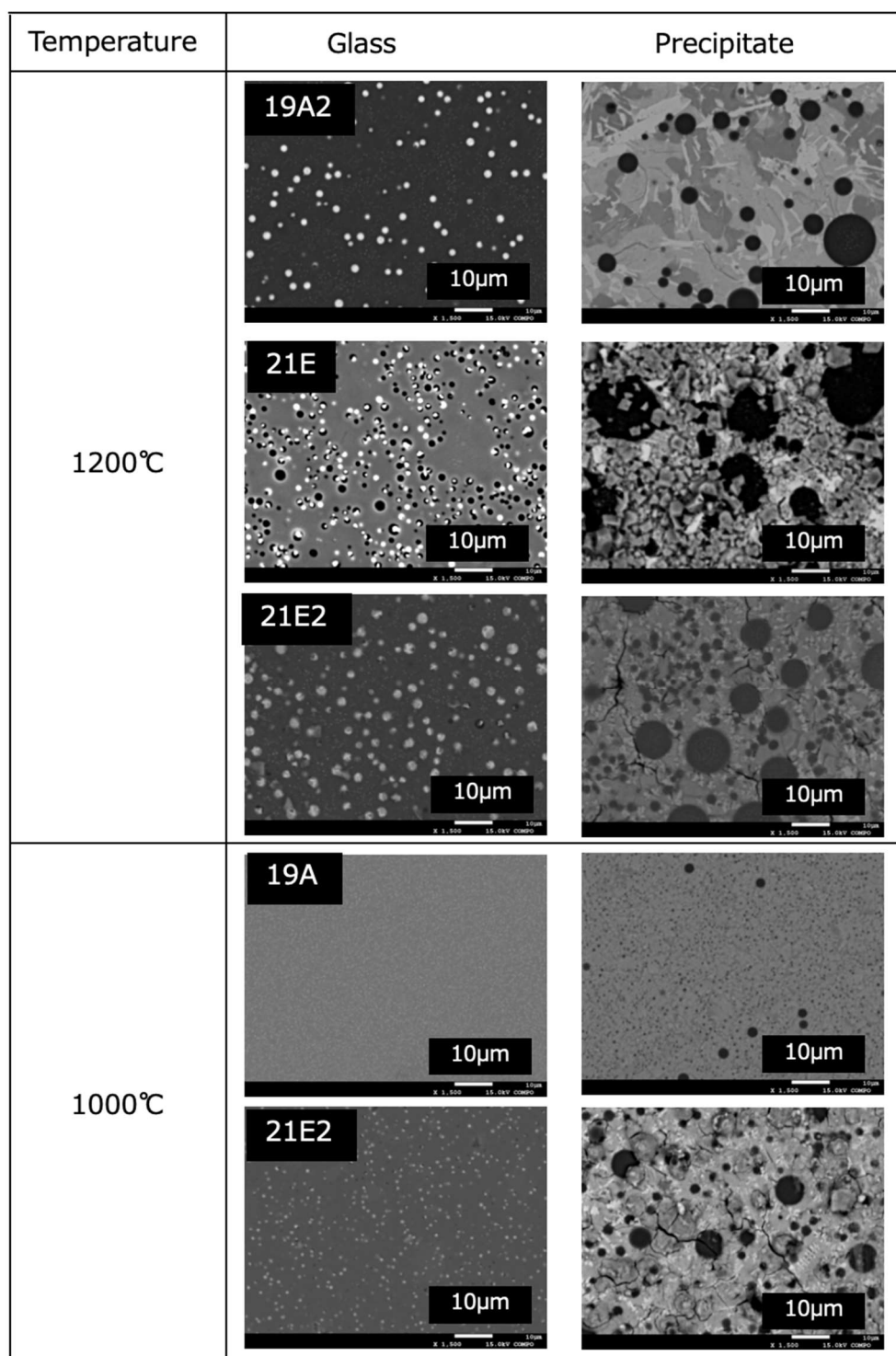


Figure 3. Backscattered electron images of glass and precipitate.

Table 4 shows the results of the mass balance calculation. The volatilization loss of B_2O_3 during the experiment was 5–8 mass%. The proportion of the phase separated molybdate phase was in the range of 22–33 mass% and the smallest in the 21E2 at 1200 °C.

The solubility of MoO_3 in the borosilicate melt was improved by the addition of V_2O_5 (Table 3). This can be discussed from the viewpoint of melt viscosity and structure.

Table 3. Chemical composition (mol%) of glass and precipitate obtained from phase equilibrium experiments. The glass composition by Lian et al. [26] is also indicated for comparison.

	Sample	Temp./°C	SiO ₂	B ₂ O ₃	Al ₂ O ₃	ZnO	CaO	Na ₂ O	Li ₂ O	V ₂ O ₅	MoO ₃
	Lian et al. [24] Vx-M2	1300	58.8	13.9	2.9	0.0	11.2	11.3	0.0	0.0–3.0	2.0
This study P	Glass	19A2	53.5	11.8	3.2	2.3	5.3	13.7	5.9	0.0	4.3
		21E	50.3	9.8	3.1	2.2	4.9	13.4	8.7	2.1	5.6
		21E2	45.7	12.3	3.1	2.2	5.3	14.5	6.1	2.3	8.6
		19A2	53.9	14.3	3.2	2.6	4.7	13.1	5.6	0.0	2.6
		21E2	48.5	15.7	3.2	2.3	4.4	13.7	5.6	2.1	4.5
		Precipitate	19A2	6.4	1.9	0.1	0.9	6.3	30.6	9.4	0.0
	21E		9.3	5.0	0.3	1.1	4.2	26.6	14.5	3.5	35.4
	21E2		6.5	2.2	0.3	1.6	7.5	28.9	9.5	6.3	37.3
	19A2		1.4	1.0	0.0	0.6	7.8	31.6	9.2	0.0	48.4
		21E2	6.4	2.2	0.3	1.6	7.4	28.7	10.2	6.2	37.0

Table 4. Results of the mass balance calculation (mass %).

Sample	Temp./°C	Silicate Phase	Molybdata Phase	B ₂ O ₃ -Loss	Residual
19A2	1200	64.3	29.3	6.4	0.55
21E		63.6	30.3	6.1	1.63
21E2		69.0	22.7	8.4	1.15
19A2	1000	64.4	31.0	4.6	0.76
21E2		60.2	33.2	6.6	1.90

In general, it is known that the MoO₃ solubility in silicate melts increases as the degree of polymerization of the melt decreases. For example, MoO₃ solubility increases with increasing Na₂O/SiO₂ ratio in the SiO₂-Na₂O-MoO₃ system [31] and B₂O₃/SiO₂ ratio in sodium-borosilicate glass [19,25,28,29] and decreasing Al₂O₃ content in aluminoborosilicate glass [25,28,29]. The degree of polymerization of the silicate melt is related to the magnitude of the viscosity. Therefore, the compositional dependence of MoO₃ solubility can be roughly discussed by using melt viscosity [28,29].

The addition of a viscosity-reducing component to silicate melt leads to depolymerization of the borosilicate network and facilitates the incorporation of large-sized MoO₄²⁻ ions into the melt structure. Ferkl et al. [35] discussed the compositional dependence of the viscosity of low-level waste glass melts based on the analyses of the augmented Adam-Gibbs model. According to the report, V₂O₅ is the component that decreases the viscosity. This suggests that vanadium is the component that suppresses phase separation and increases molybdenum solubility.

Lian et al. [26] investigated the crystallization behavior of the molybdenum phase in glasses of SiO₂-B₂O₃-Al₂O₃-Na₂O-CaO-V₂O₅-MoO₃ systems quenched at 1300 °C. They reported that when the glass composition is constant, an increase in V₂O₅ suppresses powellite crystallization. The glass transition temperatures (T_g) of the glasses by Lian et al. decreased with increasing V₂O₅ content. Since T_g is approximately equal to the temperature at which the viscosity of the supercooled melt reaches 10¹² Pa·s, the decrease in T_g represents a decrease in isothermal viscosity. In other words, the conclusion of Lian et al. [26], showing the suppression of powellite by vanadium, can also be explained in terms of melt viscosity.

Spectroscopic studies on borosilicate glasses containing vanadium and molybdenum [36] indicate that MoO₄²⁻ ions coordinate preferentially with alkali ions such as Na⁺. However, when vanadium is added, the VO₄ unit associates with alkali ions, which prevents the formation of sodium molybdate and suppresses YP generation. These are consistent with our experimental results, which showed that V₂O₅-bearing glasses increase the solubility of MoO₃.

3.3. Chemical Durability Test

Figure 4 shows the normalized leaching rates of Si and B against water in each glass. The normalized leaching rate decreased sharply until 24 h later, and then the rate of decrease slowed down. The leaching rate of V_2O_5 added glasses (21E, 21E2) was higher than that of 19A2. Bead glass had the slowest leaching rate at the beginning, but it reversed after 24 h and was the fastest after 48 h.

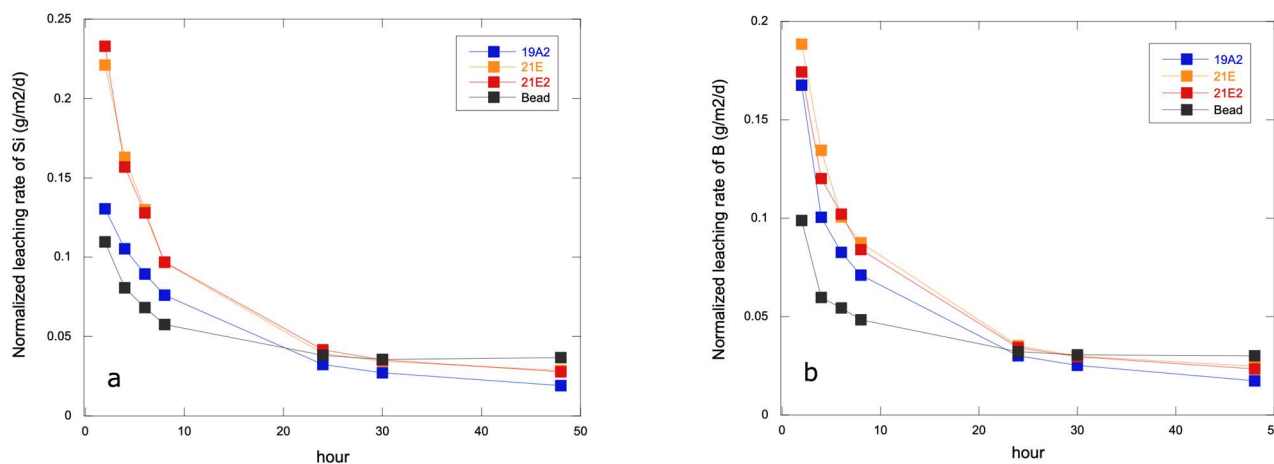


Figure 4. Normalized leaching rate of (a) Si and (b) B from glass to water as a function of time.

The leaching rate of V_2O_5 -bearing glass (21E, 21E2) was higher than that of 19A2, resulting in lower chemical durability (Figure 4). The water resistance of silicate glass is considered to be dependent on the bond strengths of the oxide components. The bond strengths are as follows: SiO_2 : 444, $BO_{3/2}$: 372, $VO_{5/2}$: 377~469, $AlO_{3/2}$: 331~423, ZnO: 301, CaO: 134, $NaO_{1/2}$: 84 and $LiO_{1/2}$: 151 (kJ/mol) [37]. The network former and intermediate components (SiO_2 , $BO_{3/2}$, $VO_{5/2}$, $AlO_{3/2}$, ZnO) show generally higher bond strengths, and the chemical durability increases with increasing proportions of these oxides. Therefore, the V_2O_5 may have improved the chemical durability, as reported by Lian et al. [26].

In this study, however, the V_2O_5 -bearing glass showed a higher normalized leaching rate. This can be attributed to differences in the ratios of components other than vanadium (Figure 4). The MCC-3 test was performed on the glass composition obtained after phase separation (F in Figure 1). The V_2O_5 -bearing glasses, 21E and 21E2, had a higher network modifier (NM)/network former (NF) ratio than that of vanadium-free glass (19A2). For this reason, it is considered that the 21E and 21E2 glasses decreased their chemical durability despite the addition of vanadium oxide.

Bead glass, which contains the simulated waste components, initially had the slowest leaching rate, but this was reversed after 24 h, and the test results showed the fastest leaching rate after 48 h (Figure 4). Figure 5 shows the normalized elemental mass loss (NL_i). The NL_i of the simulated bead glass varied linearly with time, unlike the glass without the waste component (19A2, 21E, 21E2). This result may be related to the layer formed on the contact surface by the reaction of glass and water. The reaction between glass and water initially results in the dissolution of glass. Then, the dissolution rate gradually decreases and approaches a constant rate. The slow dissolution of glasses over long periods of time is generally attributed to the saturation of silica in the solution. As the glass reacts with water, a gel layer is formed on the surface of the glass due to the repolymerization of dissolved silica. The dissolution of glass when the solution is close to saturation is thought to be prevented by the formation of a gel layer [38–43].

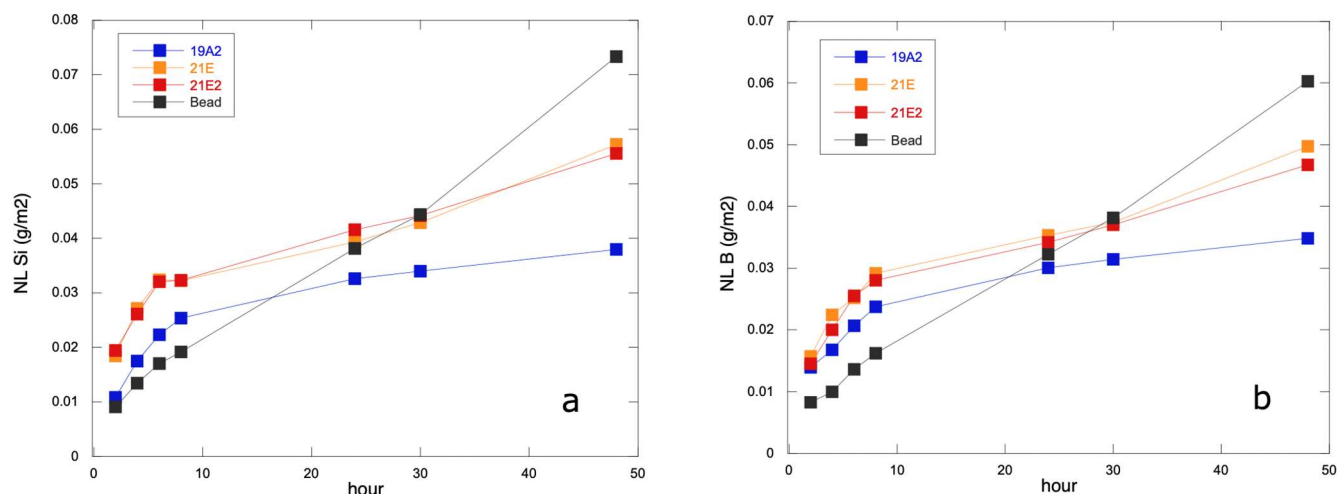


Figure 5. Normalized elemental mass loss of (a) Si and (b) B as a function of time.

Cailleteau et al. [43] carried out chemical durability tests for $\text{SiO}_2\text{-ZrO}_2\text{-B}_2\text{O}_3\text{-Na}_2\text{O-CaO}$ glasses to investigate the effect of changes in the gel structure on the leaching rate. They reported that the densification of the gel formed on the glass surface reduced the rate of alteration. It was also reported that an increase in the percentage of the insoluble element ZrO_2 in the glass suppressed the densification of the gel and increased the degree of corrosion of the glass after the experiment. In the Bead composition of this study, it is possible that the presence of the waste component prevented the formation of a gel layer at the reaction front that could inhibit glass corrosion, and that leaching continued.

4. Conclusions

In this study, phase equilibrium experiments and chemical durability tests were performed on the glasses in the system $\text{SiO}_2\text{-B}_2\text{O}_3\text{-Al}_2\text{O}_3\text{-ZnO-CaO-Na}_2\text{O-Li}_2\text{O-V}_2\text{O}_5\text{-MoO}_3$ to investigate the applicability of vanadium added glass to radioactive waste treatment.

Phase equilibrium experiments were performed at 1200 °C and 1000 °C for compositions with an excess amount of MoO_3 (13 mol%) to separate the molybdate melts. The addition of V_2O_5 suppressed the phase separation of the molybdenum phase and increased MoO_3 solubility in the borosilicate melt. This may be related to the fact that V_2O_5 causes the depolymerization of silicate melt, facilitating the incorporation of MoO_4^{2-} ions into the structure. Vanadium-bearing glass is thought to suppress the occurrence of the yellow phase in the vitrification of high-level waste.

The chemical durability tests were performed for the borosilicate glass composition obtained from the phase equilibrium experiments. No improvement in water resistance was observed due to the high network modifier/network former ratio of vanadium-bearing glass. The normalized elemental mass loss of simulated HLW glass containing waste components (Bead composition) increased linearly with time. This suggests that the waste component prevents the formation of a gel layer by reaction with water. A more detailed comparative study of the effect of vanadium addition on the chemical durability of glass is needed, considering not only the major components but also the effect of waste components.

Author Contributions: Conceptualization, M.N. and T.S.; methodology, M.N. and T.S.; formal analysis, M.N.; investigation, M.N.; resources, T.S.; writing—original draft preparation, M.N.; writing—review and editing, T.S.; supervision, T.S. All authors have read and agreed to the published version of the manuscript.

Funding: This research received no external funding.

Data Availability Statement: Raw data were generated at the Graduate School of Engineering Science, Akita University. Derived data supporting the results of this study is available from the authors upon request.

Acknowledgments: The authors would like to thank Toshiaki Ohira for his help in EPMA, ICP-AES, and XRF analysis.

Conflicts of Interest: The authors declare no conflict of interest.

References

1. Lutze, W. *Radioactive Waste Forms for the Future*; Ewing, R.C., Ed.; North-Holland: Amsterdam, The Netherlands, 1988; pp. 335–392.
2. Lutze, L. Glassy and crystalline high-level nuclear waste forms - An attempt at critical evaluation. In Proceedings of the International Symposium on Ceramics in Nuclear Waste Management, Cincinnati, OH, USA, 30 April–2 May 1979; pp. 47–51.
3. Ojovan, M.I.; Lee, W.E. Glassy Wasteforms for Nuclear Waste Immobilization. *Metall. Mater. Trans. A* **2011**, *42*, 837–851. [[CrossRef](#)]
4. Vernaza, E.T.; Bruezière, J.R.M. History of Nuclear Waste Glass in France. *Proc. Mater. Sci.* **2014**, *7*, 3–9. [[CrossRef](#)]
5. Thorpe, C.L.; Neeway, J.J.; Pearce, C.I.; Hand, R.J.; Fisher, A.J.; Walling, S.A.; Hyatt, N.C.; Kruger, A.A.; Schweiger, M.; Kosson, D.S.; et al. Forty years of durability assessment of nuclear waste glass by standard methods. *Npj Mater. Degrad.* **2021**, *5*, 61. [[CrossRef](#)]
6. Ojovan, M.I.; Lee, W.E. *New Developments in Glassy Nuclear Waste Forms*; Nova Science Publishers: New York, NY, USA, 2007.
7. McCloy, J.S.; Goel, A. Glass-ceramics for nuclear-waste immobilization. *MRS Bull.* **2017**, *42*, 233–240. [[CrossRef](#)]
8. Donald, I.W. *Waste Immobilization in Glass and Ceramic Based Hosts, Radioactive, Toxic and Hazardous Wastes*; Wiley: Chichester, UK, 2010. [[CrossRef](#)]
9. Ojovan, M.I.; Lee, W.E. *An Introduction to Nuclear Waste Immobilization*; Elsevier: Amsterdam, The Netherlands, 2005.
10. Terai, R.; Eguchi, K.; Yamanaka, H. In Proceedings of the International Symposium on Ceramics in Nuclear Waste Management, Cincinnati, OH, USA, 30 April–2 May 1979; pp. 62–65.
11. Manaktala, H.K. *An Assessment of Borosilicate Glass as a High-level Waste Form*; Nuclear Waste Regulatory Analyses: San Antonio, TX, USA, 1992; CNW 92-017.
12. Donald, I.W.; Metcalfe, B.L.; Taylor, R.N.J. The immobilization of high level radioactive wastes using ceramics and glasses. *J. Mater. Sci.* **1997**, *32*, 5851–5887. [[CrossRef](#)]
13. Goel, A.; McCloy, J.S.; Pokorny, R.; Kruger, A.A. Challenges with vitrification of Hanford High-Level Waste (HLW) to borosilicate glass—An overview. *J. Non-Cryst. Solids* **2019**, *4*, 100033. [[CrossRef](#)]
14. Mazurin, O.V.; Porai-Koshits, E.A. *Phase Separation in Glass*; North-Holland: Amsterdam, The Netherlands, 1984. [[CrossRef](#)]
15. Lee, W.E.; Ojovan, M.I.; Stennett, M.C.; Hyatt, N.C. Immobilisation of radioactive waste in glasses, glass composite materials and ceramics. *Adv. Appl. Ceram.* **2006**, *105*, 3–12. [[CrossRef](#)]
16. Nicoleau, E.; Schuller, S.; Angeli, F.; Charpentier, T.; Jollivet, P.; Alexandre, L.G.; Fournier, M.; Mesbah, A.; Vasconcelos, F. Phase separation and crystallization effects on the structure and durability of molybdenum borosilicate glass. *J. Non-Cryst. Solids* **2015**, *427*, 120–133. [[CrossRef](#)]
17. Kroeker, S.; Schuller, S.; Wren, J.E.C.; Greer, B.J.; Mesbah, A. ^{133}Cs and ^{23}Na MAS NMR spectroscopy of molybdate crystallization in model nuclear glasses. *J. Am. Ceram. Soc.* **2016**, *99*, 1557–1564. [[CrossRef](#)]
18. Yamane, M.; Nakao, Y. Phase separation in the glass containing high level radioactive waste. *Yogyo-Kyokai-Shi* **1979**, *87*, 328–332. [[CrossRef](#)]
19. Caurant, D.; Majérus, O.; Fadel, E.; Lenoir, M.; Gervais, C.; Pinet, O. Effect of molybdenum on the structure and on the crystallization of $\text{SiO}_2\text{-Na}_2\text{O-CaO-B}_2\text{O}_3$ Glasses. *J. Am. Ceram. Soc.* **2007**, *90*, 774–783. [[CrossRef](#)]
20. Magnin, M.; Schuller, S.; Caurant, D.; Majérus, O.; Ligny, D.D.; Mercier, C. Effect of compositional changes on the structure and crystallization tendency of a borosilicate glass containing MoO_3 . *Ceram. Trans. Ser.* **2009**, *13*, 59–67.
21. Chouard, N.; Caurant, D.; Majérus, O.; Dussossoy, J.L.; Ledieu, A.; Peugot, S.; Hadjean, R.B.; Ramos, J.P.P. Effect of neodymium oxide on the solubility of MoO_3 in an aluminoborosilicate glass. *J. Non-Cryst. Solids* **2011**, *357*, 2752–2762. [[CrossRef](#)]
22. Taurines, T.; Boizot, B. Microstructure of powellite-rich glass-ceramics: A model system for high level waste immobilization. *J. Am. Ceram. Soc.* **2012**, *95*, 1105–1111. [[CrossRef](#)]
23. Chouard, N.; Caurant, D.; Majérus, O.; Guezi-Hasni, N.; Dussossoy, J.L.; Baddour-Hadjean, R.; Pereira-Ramos, J.P. Thermal stability of $\text{SiO}_2\text{-B}_2\text{O}_3\text{-Al}_2\text{O}_3\text{-Na}_2\text{O-CaO}$ glasses with high Nd_2O_3 and MoO_3 concentrations. *J. Alloys Compd.* **2016**, *671*, 84–99. [[CrossRef](#)]
24. Brehault, A.; Patil, D.; Kamat, H.; Youngman, R.E.; Thirion, L.M.; Mauro, J.C.; Corkhill, C.L.; McCloy, J.S.; Goel, A. Compositional Dependence of Solubility/Retention of Molybdenum Oxides in Aluminoborosilicate-Based Model Nuclear Waste Glasses. *J. Phys. Chem. B* **2018**, *122*, 1714–1729. [[CrossRef](#)]
25. Sugawara, T.; Ohira, T.; Oowak, K.; Kanehira, N. Thermodynamic optimization of phase separation of molybdenum phase in high-level waste glass. In Proceedings of the ICG Annual Meeting, Yokohama, Japan, 23–28 September 2018. ICGY037.
26. Lian, Q.; Zhang, X.; Ji, H.; Yu, P.; Guo, X.; Wan, W.; Liu, H.; Zheng, K.; Zhu, Y.; Wang, H.; et al. Effect of V_2O_5 on crystallization tendency and chemical durability of Mo-bearing aluminoborosilicate glass. *Mater. Res. Express* **2020**, *7*, 045201. [[CrossRef](#)]
27. Zhou, J.; Liao, Q.; Wang, F.; Wang, Y.; Zhu, H.; Zhu, Y. Effect of Na_2O and CaO on the solubility and crystallization of Mo in borosilicate glasses. *J. Non-Cryst. Solids* **2021**, *557*, 120623. [[CrossRef](#)]

28. Sugawara, T.; Ohira, T.; Oowak, K.; Tsukada, T. International Year of Glass 2022; Future prospects of glass science in the reprocessing process: (3) The reaction behavior of Molybdenum in a glass melter: Recent progress. In Proceedings of the Atomic Energy Society of Japan, Annual Meeting, Online, 16–18 March 2022. 3L_PL03.
29. Sugawara, T.; Ohira, T.; Sekine, A.; Adachi, M.; Sato, H. Crystallization of molybdenum oxide phase from simulated high-level waste glass under slow cooling. *J. Ceram. Soc. Jpn.* **2020**, *130*, 933–942. [[CrossRef](#)]
30. Manara, D.; Grandjean, A.; Pinet, O.; Dussossoy, J.L.; Neuville, D.R. Sulfur behavior in silicate glasses and melts: Implications for sulfate incorporation in nuclear waste glasses as a function of alkali cation and V₂O₅ content. *J. Non-Cryst. Solids* **2007**, *353*, 12–23. [[CrossRef](#)]
31. Stempok, M.; Voldan, J. Homogenous silicate glasses in systems Na₂O-SiO₂-WO₃ and Na₂O-SiO₂-MoO₃. *Ceramics-Silikaty* **1974**, *18*, 19–30.
32. Uruga, K.; Tsukada, T.; Usami, T. Generation mechanism and prevention method of secondary molybdate phase during vitrification of PUREX wastes in liquid-fed ceramic melter. *J. Nucl. Sci. Technol.* **2020**, *57*, 433–443. [[CrossRef](#)]
33. Schuller, S.; Gosse, S.; Rogez, J. Glass, crystallization and phase separation: An insight into glass enriched in MoO₃. In Proceedings of the Joint ICTP-IAEA Workshop on Fundamentals of Vitrification and Vitreous Materials for Nuclear Waste Immobilization (smr 3159), Trieste, Italy, 6–10 November 2017; cea-02400187.
34. Buekers, J.; Mertens, J.; Smolders, E. Toxicity of the molybdate anion in soil is partially explained by effects of the accompanying cation or by soil pH. *Environ. Toxicol. Chem.* **2010**, *29*, 1274–1278. [[CrossRef](#)] [[PubMed](#)]
35. Ferkl, P.; Hrma, P.; Kruger, A.A. Augmented Adam-Gibbs model for glass melt viscosity and configuration entropy as functions of temperature and composition. *J. Non. Cryst. Solids* **2022**, *595*, 121832. [[CrossRef](#)]
36. Suzuki, M.; Umesaki, N.; Tanaka, T.; Ohkubo, T.; Kakihara, T.; Hashimoto, T.; Kawashima, H. Structural behaviour of vanadium ions in alkali borosilicate glass for nuclear waste storage. *Phys. Chem. Glasses B* **2018**, *59*, 181–192. [[CrossRef](#)]
37. Sun, K.H. Fundamental condition of glass formation. *J. Am. Chem. Soc.* **1947**, *30*, 277–281. [[CrossRef](#)]
38. Grambow, B. Corrosion of glass. In *Uhlig's Corrosion Handbook*, 2nd ed.; Revie, R.W., Ed.; Wiley: Chichester, UK, 2000; pp. 411–437.
39. Barkatt, A.; Macedo, P.B.; Gibson, B.C.; Montrose, C.J. Modelling of waste performance and system release. *Mater. Res. Soc. Symp. Proc.* **1984**, *44*, 3–13. [[CrossRef](#)]
40. Delage, F.; Ghaleb, D.; Dussossoy, J.L. A mechanistic model for understanding nuclear waste glass dissolution. *J. Nucl. Mater.* **1992**, *190*, 191–197. [[CrossRef](#)]
41. Xing, S.B.; Buechele, A.C.; Pegg, I.L. Effect of surface layers on the dissolution of nuclear waste glasses. *Mater. Res. Soc. Symp. Proc.* **1994**, *333*, 541–548. [[CrossRef](#)]
42. Gin, S.; Ribet, I.; Couillard, M. Role and properties of the gel formed during nuclear glass alteration: Importance of gel formation conditions. *J. Nucl. Mater.* **2001**, *298*, 1–10. [[CrossRef](#)]
43. Cailleteau, C.; Angeli, F.; Devreux, F.; Gin, S.; Jestin, J.; Jollivet, P.; Spalla, O. Insight into Silicate-Glass Corrosion Mechanisms. *Nat. Mater.* **2008**, *7*, 978–983. [[CrossRef](#)]

Disclaimer/Publisher's Note: The statements, opinions and data contained in all publications are solely those of the individual author(s) and contributor(s) and not of MDPI and/or the editor(s). MDPI and/or the editor(s) disclaim responsibility for any injury to people or property resulting from any ideas, methods, instructions or products referred to in the content.